Analytic expressions for the inelastic scattering and energy loss of electron and proton beams in carbon nanotubes

D. Emfietzoglou,[1,a)] I. Kyriakou,[1] R. Garcia-Molina,[2] I. Abril,[3] and K. Kostarelos[4]
[1]*Medical Physics Laboratory, University of Ioannina Medical School, 45110 Ioannina, Greece*
[2]*Departamento de Física–CIOyN, Universidad de Murcia, E-30100 Murcia, Spain*
[3]*Departament de Física Aplicada, Universitat d'Alacant, E-03080 Alacant, Spain*
[4]*Nanomedicine Laboratory, Centre for Drug Delivery Research, School of Pharmacy, University of London, London WC1N 1AX, United Kingdom*

(Received 14 May 2010; accepted 14 June 2010; published online 3 September 2010)

We have determined "effective" Bethe coefficients and the mean excitation energy of stopping theory (*I*-value) for multiwalled carbon nanotubes (MWCNTs) and single-walled carbon nanotube (SWCNT) bundles based on a sum-rule constrained optical-data model energy loss function with improved asymptotic properties. Noticeable differences between MWCNTs, SWCNT bundles, and the three allotropes of carbon (diamond, graphite, glassy carbon) are found. By means of Bethe's asymptotic approximation, the inelastic scattering cross section, the electronic stopping power, and the average energy transfer to target electrons in a single inelastic collision, are calculated *analytically* for a broad range of electron and proton beam energies using realistic excitation parameters. © *2010 American Institute of Physics*. [doi:10.1063/1.3463405]

I. INTRODUCTION

Beams of charged particles (i.e., electrons, protons, or heavier ions) represent an established tool for the controlled modification of materials and have already been used for tailoring the physical and chemical properties of carbon nanotubes (CNTs) (Refs. 1 and 2) representing, in effect, another postsynthetic, "constructive destruction" sorting approach.[3] However, in order to optimize the use of charged-particle beams and to predict radiation damage in space or nuclear technology applications, it is important that their interactions with CNTs are well understood and accurately quantified. Most studies so far have concentrated on the nuclear stopping of CNTs due to the elastic scattering of charged particles by target atoms leading to knock-on displacement of carbon atoms from the CNT lattice.[4] This is the dominant radiation damage mechanism for slow ions below ~10 keV/u and electrons above the CNT knock-on threshold of ~80 keV.[5] In contrast, little is known on the electronic stopping of CNTs due to the inelastic scattering of charged particles by target electrons, despite the fact that electronic excitations can effectively mediate materials modification and cause radiation damage through (mainly) beam-stimulated local chemical reactions.[2,5]

There exist several recent theoretical studies of the electronic energy loss of charged particles in CNTs.[6–15] The approaches can be divided to those using Bloch's hydrodynamic approximation[6–9] and those employing the dielectric response theory either in the Bohm–Pines random-phase-approximation[10,11] or in the semiclassical Drude approximation.[12–15] Both approaches have been successfully applied to a variety of low-dimensional systems and carbon nanostructures, in particular. Dielectric models are known to be particularly effective in describing plasmon excitations in an electron gas whereas hydrodynamic models, although perhaps more qualitative in some respects, are capable of handling boundary effects due to the presence of different dielectric media. However, due to the considerable amount of numerical work involved, both approaches are usually restricted to the study of individual CNTs [most often isolated single-walled CNTs (SWCNTs)]. Thus, for practical calculations and data analysis concerning the irradiation of bulk CNT systems (e.g., bundles) or macroscopic samples (e.g., thin films) one would wish to have a simpler approach of wider applicability valid over a broad energy range of the incident charged particle. Due to the absence of such a simple model, bulk graphite excitation properties are commonly used for describing the inelastic interaction between the charged-particle beam and the CNT.

The aim of the present work is to provide realistic excitation parameters for multiwalled CNTs (MWCNTs) and SWCNT bundles in order to enable the inelastic scattering cross section, the electronic stopping power, and the average energy transfer to target electrons in a single inelastic collision to be calculated analytically as a function of charged-particle beam energy. This is accomplished within the theoretical framework of the Bethe theory.[16] Compared to previously used methods,[6–15] the main advantage of the Bethe theory is that it offers the possibility of expressing the above magnitudes in a strikingly simple analytic form applicable over a wide range of beam energies within, of course, the limits of validity of the plane-wave Born approximation (PWBA). Thus, it is feasible using a simple method to address practical problems associated, for example, with irradiation experiments using kiloelectron volt electron beams from scanning electron microscope or transmission electron microscope and megaelectron volt protons relevant to space applications. For economy of space all expressions are given in their nonrelativistic form and, therefore, pertain to the longitudinal part of the interaction. In their present nonrelativ-

a)Electronic mail: demfietz@cc.uoi.gr.

 © 2010 American Institute of Physics

Downloaded 04 Sep 2010 to 195.130.120.61. Redistribution subject to AIP license or copyright; see http://jap.aip.org/about/rights_and_permissions

istic form, they can be safely used up to a few tens of kilo-electron volt (megaelectron volt) electron (proton) energies. However, if needed, their relativistic extension is straightforward.[16]

II. INELASTIC CROSS SECTIONS

The Bethe theory provides an asymptotic expansion for the inelastic scattering cross section of PWBA in powers of T^{-1} (T is proportional to the square of the charged-particle velocity) with coefficients that depend solely on materials properties. Hereafter the use of the Bethe asymptotic expansion to T^{-1} order will be called the Bethe approximation. Then, the probability per unit path length that a (nonrelativistic) charged particle will transfer energy W to the target can be expressed in the Bethe approximation as follows:

$$P_W(\mathrm{eV}^{-1}\ \mathrm{nm}^{-1}) = 3.01\ \mathrm{Im}\{-1/\varepsilon_W\}T(\mathrm{eV})^{-1}\ln\{c_W T(\mathrm{eV})/\mathrm{Ry}\}, \tag{1}$$

where Ry is the Rydberg constant, $T=mv^2/2$ with m being the electron rest mass and v the projectile velocity, and ε_W is the dielectric response function of the target at vanishing momentum transfer or optical limit ($q\approx 0$). The value of the constant on the right-hand-side of Eq. (1) comes from: $(2\pi a_0)^{-1}=3.01\ \mathrm{nm}^{-1}$ where a_0 is the Bohr radius. Note that, in the present units, the P_W of Eq. (1) is equivalent to the differential inverse inelastic mean free path. The $\mathrm{Im}\{-1/\varepsilon_W\}$ is the so-called energy loss-function (ELF), also at the optical limit, which describes the excitation spectrum of the material by inelastic charged-particle scattering at nearly forward angles. The Bethe coefficient c_W is a complicated function of W that depends on the value of ELF at finite q and, generally, is of the order of unity.[16] Evidently, the use of Eq. (1) depends upon the evaluation of $\mathrm{Im}\{-1/\varepsilon_W\}$ and c_W which are both excitation properties of the material independent of the charge, velocity, or mass of the particle.

Although the dielectric response of individual CNTs is anisotropic (like graphite), for random (nonparaxial) charged particle trajectories both the in-plane and out-of-plane excitations are involved due to the cylindrical geometry. In this case, the use of a macroscopic (continuum) dielectric response function, as the one employed here, seems justified. Obviously, this approximation will also suffice for bulk or macroscopic samples containing nonaligned CNTs (e.g., bundles). More generally, the present approach should be reasonably valid for those cases where the contribution of in-plane and out-of-plane excitations is comparable, e.g., as in angle-integrated electron-energy loss spectroscopy (EELS).[17] To determine the $\mathrm{Im}\{-1/\varepsilon_W\}$ of the examined CNT systems over the broad excitation range relevant to the inelastic interaction of energetic charged-particle beams, we proceed as follows. Due to the large energy difference between valence-electron and core-electron excitations, the total ELF (at $q\approx 0$) can be approximated by the following sum: $\mathrm{Im}\{-1/\varepsilon_W\}\approx \mathrm{Im}\{-1/\varepsilon_W\}_{\mathrm{v}}+\mathrm{Im}\{\varepsilon_W\}_{\mathrm{K}}$, where "v" and "K" denote the valence and K-shell contributions, respectively. As first suggested by Powell,[18] the valence contribution to the ELF, $\mathrm{Im}\{-1/\varepsilon_W\}_{\mathrm{v}}$, can be derived from experimental optical data which ensure a realistic, material-specific representation of the excitation spectrum. In the present work we adopt our previously developed Drude parameterization[19] of the experimental EELS data measured from relatively thick MWCNTs (~21–44 walls and 13–34 nm in diameter)[20] and large SWCNT bundles[21] over the valence excitation range (~0–50 eV). *Ab initio* time-dependent density-functional-theory calculations[22] of the ELF of SWCNTs at vanishing momentum transfer (optical limit) over the valence excitation range have confirmed the general characteristics of the EELS data.[21] In particular, it was shown that at the long length scales associated with the optical limit the position of the $\pi+\sigma$ plasmon peak, the main energy-loss channel of the system, sensitively depends upon screening effects due to intertube interactions. These screening effects lead to a shift of the peak to higher energy losses and a pronounced difference between $\mathrm{Im}\{-1/\varepsilon_W\}_{\mathrm{v}}$ and the optical absorption spectrum, $\mathrm{Im}\{\varepsilon_W\}_{\mathrm{v}}$. As expected, this difference vanishes for nearly isolated tubes at large intertube separations where $\mathrm{Im}\{-1/\varepsilon_W\}_{\mathrm{v}}\rightarrow \mathrm{Im}\{\varepsilon_W\}_{\mathrm{v}}$.

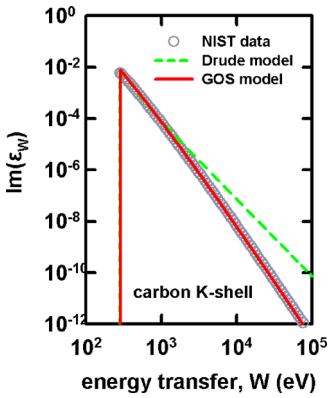

FIG. 1. (Color online) The carbon's K-shell contribution to the ELF in the optical limit under the approximation: $\mathrm{Im}\{-1/\varepsilon_W\}_{\mathrm{K}}\approx \mathrm{Im}\{\varepsilon_W\}_{\mathrm{K}}$. Full-lines correspond to the present hydrogenic GOS model, broken lines to the Drude model of Ref. 19 and symbols to NIST data taken from Ref. 25.

For the K-shell contribution which sets in at ~285 eV (approximately the carbon K-edge) and for which the approximation $\mathrm{Im}\{-1/\varepsilon_W\}_{\mathrm{K}}\approx \mathrm{Im}\{\varepsilon_W\}_{\mathrm{K}}$ safely holds, we improve upon our previous calculation[19] using the relation $\mathrm{Im}\{\varepsilon_W\}_{\mathrm{K}}=\mathrm{const.}(N/Z)W^{-1}(\xi df_{\mathrm{K}}^{\mathrm{H}}/dW)$ where const. $=8\pi^2 a_0^3\mathrm{Ry}^2$, N,Z are the target electronic density and atomic number, respectively, $df_{\mathrm{K}}^{\mathrm{H}}/dW$ is the optical limit of the scaled hydrogenic generalized-oscillator-strength (GOS) of carbon,[23] and $\xi=1.026$ is a normalization factor deduced from first-principles atomic calculations.[24] In Fig. 1 it is clearly shown that the present model for the K-shell significantly improves the asymptotic behavior at large W of the Drude K-shell model used previously,[19] as judged from the comparison with the x-ray data from the National Institute of Standards and Technology (NIST).[25] We should note that any variation in the shape of the carbon K-edge in different carbon structures[26] is too small to be of any significance for the present calculations where the magnitudes of interest depend mainly upon integrals of the ELF over a broad excitation range.

The overall internal consistency of our ELF model is tested by two important sum rules,[27] namely, the Kramers–

Downloaded 04 Sep 2010 to 195.130.120.61. Redistribution subject to AIP license or copyright; see http://jap.aip.org/about/rights_and_permissions

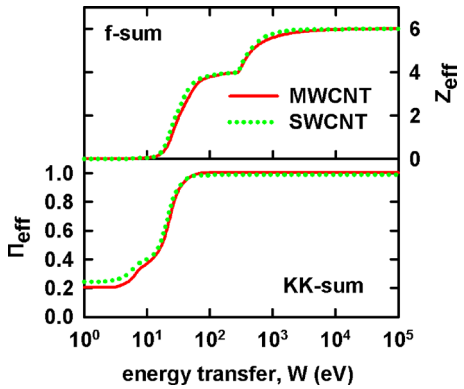

FIG. 2. (Color online) The *f*-and KK-sum rules for the present ELFs, $\mathrm{Im}\{-1/\varepsilon_W\}$, for MWCNTs and SWCNT bundles.

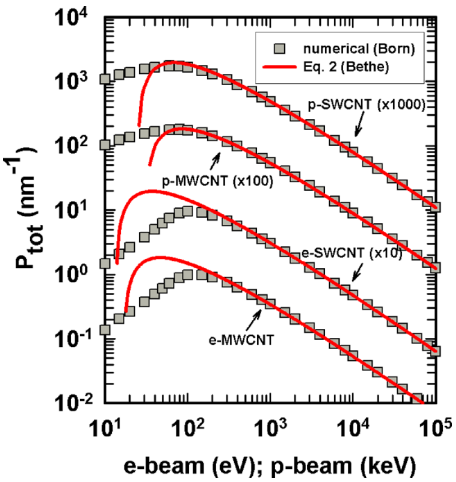

FIG. 3. (Color online) Comparison of total inelastic scattering cross section (P_{tot}) calculations for electron (e) and proton (p) beam irradiation of MWCNTs and SWCNT bundles: Full-lines correspond to Eq. (2) with the values of the Bethe coefficients: $b_{\mathrm{tot}}=27.9$ eV and $c_{\mathrm{tot}}=0.80$ for MWCNTs, and $b_{\mathrm{tot}}=23.9$ eV and $c_{\mathrm{tot}}=0.88$ for SWCNT bundles. Symbols correspond to numerical results from PWBA using the optical-data model for the momentum-dependent ELF of Ref. 19 and the present hydrogenic GOS model for the K-shell.

Krönig (KK) and *f*-sum rules that read, respectively, $\Pi_{eff}=(2/\pi)\int_0^W W'^{-1}\,\mathrm{Im}\{-1/\varepsilon_{W'}\}dW'+\mathrm{Re}\{1/\varepsilon_{W=0}\}$, where $\mathrm{Re}\{1/\varepsilon_{W=0}\}\equiv 1/\varepsilon_1$ with ε_1 being the limiting value of ε_W as $W\to 0$, and $Z_{eff}=(2Z/\pi E_{\mathrm{p}}^2)\int_0^W W'\,\mathrm{Im}\{-1/\varepsilon_{W'}\}dW'$, where $E_{\mathrm{p}}=\hbar\sqrt{4\pi Ne^2/m}$ is the free-electron plasmon energy of the material. From the EELS data[20,21] for the two systems examined we deduce the values: $E_{\mathrm{p}}=27.8$ eV and $\varepsilon_1=4.88$ for MWCNTs, and $E_{\mathrm{p}}=24.4$ eV and $\varepsilon_1=4.09$ for SWCNT bundles. It is important that both sum rules are satisfied because, as it is apparent from their definition as well as from Fig. 2, the value of Π_{eff} is sensitive to small W (below ~50 eV) whereas that of Z_{eff} to intermediate and large W(~50–5000 eV). Thus, in effect, the KK and *f*-sum rules are complementary. As shown in Fig. 2, for $W\to\infty$ we obtain (to better than 1%) the correct limiting values $Z_{eff}\approx 6$ and $\Pi_{eff}\approx 1$.

The form of Eq. (1) suggests that $\mathrm{Im}\{-1/\varepsilon_W\}$ suffices at the limit of large T where P_W goes asymptotically as $T^{-1}\ln(T)$. To go beyond the optical approximation the coefficient c_W, associated with finite q features in the ELF, must be determined. However, since an analytic expression for c_W is not feasible, we adopt an approximate procedure and determine an "effective" Bethe coefficient c_{tot} (independent of W) from the relation $P_{\mathrm{tot}}=\int P_W dW$, where P_{tot} is the total inelastic scattering cross section in dimensions of inverse length (equivalent to the inverse inelastic mean free path). The P_{tot} is calculated numerically within the PWBA where the key material property is the *momentum-dependent* ELF. The latter is calculated from the present $\mathrm{Im}\{-1/\varepsilon_W\}$ extended to arbitrary q values by semiempirical dispersion relations[19] and the analytic properties of the GOS model.[23] The use of extended optical-data models is known to give reasonably accurate results within the range of validity of PWBA, as exemplified by the widespread usage[28,29] of the Penn[30] and Ashley[31] models (among others[32,33]). In the present work, however, we go beyond the standard dispersion approximations for unbound (infinite) media by accounting for finite-size and linewidth broadening effects in CNTs as discussed in Ref. 19. The values of c_{tot} which provide the best overall fit to the numerical P_{tot} data are $c_{\mathrm{tot}}=0.80$ for MWCNTs and $c_{\mathrm{tot}}=0.88$ for SWCNT bundles. Both values are considerably lower than the corresponding values found for the three allotropes of carbon using Penn's algorithm:[34] $c_{\mathrm{tot}}=1.415$ for diamond, $c_{\mathrm{tot}}=1.59$ for graphite, and $c_{\mathrm{tot}}=1.59$ for glassy carbon. Having determined c_{tot}, it is then straightforward using Eq. (1) to obtain an *analytic* expression for P_{tot} as a function of beam energy in the Bethe approximation:

$$P_{\mathrm{tot}}(\mathrm{nm}^{-1})=3.01T(\mathrm{eV})^{-1}b_{\mathrm{tot}}(\mathrm{eV})\ln\{c_{\mathrm{tot}}T(\mathrm{eV})/\mathrm{Ry}\},\qquad(2)$$

where the Bethe coefficient $b_{\mathrm{tot}}=\int_0^\infty \mathrm{Im}\{-1/\varepsilon_W\}dW$ depends upon an integral over the complete ELF at $q\approx 0$. Using the present $\mathrm{Im}\{-1/\varepsilon_W\}$ we obtain $b_{\mathrm{tot}}=27.9$ eV for MWCNTs and $b_{\mathrm{tot}}=23.9$ eV for SWCNT bundles. In terms of the perhaps more familiar dipole-matrix-elements squared (for all electronic excitations) $M_{\mathrm{tot}}^2=(2\mathrm{RyZ}/\pi E_{\mathrm{p}}^2)b_{\mathrm{tot}}$, we obtain $M_{\mathrm{tot}}^2=1.88$ for MWCNTs and $M_{\mathrm{tot}}^2=2.09$ for SWCNT bundles. In comparison, the corresponding values for the three allotropes of carbon determined also from experimental optical data are:[34] $M_{\mathrm{tot}}^2=1.552$ for diamond, $M_{\mathrm{tot}}^2=2.038$ for graphite, and $M_{\mathrm{tot}}^2=1.690$ for glassy carbon. From inspection of Eq. (2) it is seen that the magnitude of P_{tot} for $T/\mathrm{Ry}\gg c_{\mathrm{tot}}$ is determined primarily by the value of b_{tot} (or M_{tot}^2) while the details of its energy variation at not too large T will depend upon c_{tot}.[35]

In Fig. 3 we compare the results obtained from the analytic Bethe expression, Eq. (2), against the numerical calculations of P_{tot} in the PWBA as described above. It is clear from Fig. 3 that the above determined values for the Bethe coefficients, b_{tot} and c_{tot}, render Eq. (2) in good agreement with the numerical data almost down to the cross section maximum. Specifically, for electrons the difference between the analytic and numerical results is less than ~3% above 500 eV rising to 10%–15% at 200 eV, whereas for protons it is less than 3% above 100 keV. Thus, Eq. (2) with the present Bethe coefficients can be safely used almost over the full range of validity of the PWBA. For extending further the application of Eq. (2) to even lower T one would need to determine P_{tot} to the order T^{-2}. However, due to the inherent limitations of the PWBA, the uncertainty associated with the

Downloaded 04 Sep 2010 to 195.130.120.61. Redistribution subject to AIP license or copyright; see http://jap.aip.org/about/rights_and_permissions

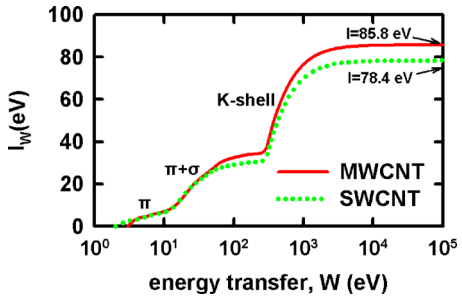

FIG. 4. (Color online) Cumulative mean excitation energy of MWCNTs and SWCNT bundles calculated by Eq. (4).

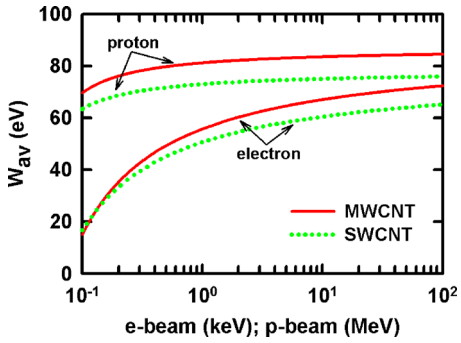

FIG. 5. (Color online) Average energy transfer in a single inelastic collision to the electronic subsystem of MWCNTs and SWCNT bundles as a function of electron (e) and proton (p) beam energy calculated from Eq. (5).

numerical P_{tot} values below the maximum increases rapidly so the usefulness of such an effort is questionable. Also, it should be pointed out that the conventional determination of c_{tot} through a Fano plot analysis of the high-energy asymptotic Bethe region would have naturally restricted the reliability of Eq. (2) to significantly higher beam energies. In contrast, with the present approach, Eq. (2) is now useful over a broader energy range. Although relativistic corrections to the electron calculations can amount to ~10%–20% in the range 30–100 keV, the inclusion of such corrections is inconsequential here since they will apply equally to both the Bethe and PWBA calculations.

III. ELECTRONIC ENERGY LOSS

The Bethe asymptotic expansion holds for any momentum integrated cross section. Then, in the Bethe approximation (i.e., to order T^{-1}) the electronic stopping power, defined as the mean energy loss per unit path length due to inelastic collisions with target electrons, can be expressed in the following analytic form:

$$S(\text{eV/nm}) = 13.0N(\text{e/nm}^3)T(\text{eV})^{-1}\ln\{aT(\text{eV})/I(\text{eV})\}, \quad (3)$$

where $a=1.166$ for electrons and $a=4$ for protons. The value of the constant on the right-hand-side of Eq. (3) comes from: $8\pi a_0^2\text{Ry}^2 = 13.0(\text{nm eV})^2$. The I-value or *mean excitation energy* of the material is the only nontrivial parameter in Eq. (3) defined by an energy-weighted integral over the ELF as follows:

$$I \equiv \lim_{W\to\infty} \exp\left\{\frac{\int_0^W W' \ln(W')\text{Im}\{-1/\varepsilon_{W'}\}dW'}{\int_0^W W' \text{Im}\{-1/\varepsilon_{W'}\}dW'}\right\}. \quad (4)$$

A plot of the exponential on the right-hand-side of Eq. (4), or cumulative mean excitation energy, I_W, is presented in Fig. 4. Clearly, as found for other materials, the limiting value of I_W is reached at relatively high W (at least approximately ten times the K-edge) with the K-shell having the dominant contribution due to its large binding energy.[36] This realization has two effects: first, it makes the I-value particularly sensitive to the model used for $\text{Im}\{\varepsilon_W\}_K$ and, second, restricts the reliability of Eq. (3) to values of T much larger than the K-edge, unless it is supplemented by a so-called shell-correction term (of order T^{-2}) related to the q-dependence of ELF

For $W\to\infty$ we obtain $I=85.8$ eV for MWCNTs and $I=78.4$ eV for SWCNT bundles. Since the I-value depends upon the spectral distribution of $\text{Im}\{-1/\varepsilon_W\}$, the larger I-value for MWCNT is consistent with the observation of a blueshift in the plasmon energy with increasing number of walls.[37] In comparison, the ICRU (Ref. 38) recommended value for graphite is $I=78$ eV while recent estimates for the three allotropes of carbon based on experimental optical data give:[39] $I=89.4$ eV for diamond, $I=76.5$ eV for graphite, and $I=102.5$ eV for glassy carbon. Although a difference in the I-value of the order of 10 eV has a relatively small influence on the magnitude of S (for $T \gg I$) it can still have important practical consequences due to its impact on the absolute magnitude of the penetration range and, accordingly, on the depth-dose profile (and the Bragg peak position in proton beam irradiation) over distances comparable to the dimensions of the irradiated CNT systems.

The average energy transfer, W_{av}, to the electronic subsystem of CNTs in a *single* inelastic collision can also be calculated analytically within the Bethe approximation from:

$$W_{av} = \frac{S}{P}, \quad (5)$$

where $P \equiv P_{\text{tot}}$ and S are obtained from Eqs. (2) and (3), respectively. Recently, W_{av} has been shown to be an important parameter for understanding the role of electronic excitations in the microscopic mechanism of defect production in CNTs by charged-particle beams.[40] A plot of W_{av} as a function of beam energy is presented in Fig. 5.

Interestingly, the observed difference of 5–10 eV between MWCNTs and SWCNT bundles is comparable to the postulated threshold for "direct" inelastic damage to CNTs.[41,42] A difference of several electron volts can also have important consequences to secondary electron emission applications.[43–45]

IV. CONCLUSION

In the present work, we have determined "effective" Bethe coefficients (b_{tot}, c_{tot}) and the mean excitation energy (I-value) of stopping power theory for MWCNTs and SWCNT bundles based on an improved ELF model deduced from experimental optical data for valence-electron excitations and atomic properties for core-electron excitations. Noticeable differences between MWCNTs, SWCNT bundles, and the three allotropes of carbon (diamond, graphite, glassy

Downloaded 04 Sep 2010 to 195.130.120.61. Redistribution subject to AIP license or copyright; see http://jap.aip.org/about/rights_and_permissions

carbon) are found. The above excitation parameters enable, within Bethe's asymptotic approximation, the inelastic scattering cross section, the electronic stopping power, and the average energy transfer to the electronic subsystem in a single inelastic collision to be calculated *analytically* for a broad range of electron and proton beam energies. Using the simple z^2-scaling (where z is the charge of the particle) of the PWBA, the expressions can also be used for other light ions (e.g., α-particles). Moreover, due to their simplicity and analytic properties they can be directly usable for Monte Carlo simulation of the inelastic interactions of kiloelectron volt electron and megaelectron volt proton beams in bulk, macroscopic samples containing MWCNTs or SWCNT bundles. It is also envisioned that, by employing excitation parameters specific to CNTs, the present expressions would provide a more realistic model for the inelastic interaction of charged-particle beams with CNTs and thus, improve upon the widely used practice of using beam-bulk graphite interaction models.

ACKNOWLEDGMENTS

We thank A. V. Krasheninnikov and C. J. Powell for making critical and useful comments on the manuscript. In addition, we thank C. J. Powell for kindly providing to us the latest values of the excitation parameters for the three allotropes of carbon used for comparision. Financial support for D.E., I.K., and K.K. by the European Union FP7 ANTICARB (Grant No. HEALTH-F2-2008-201587) is acknowledged.

[1]A. V. Krasheninnikov and F. Banhart, Nature Mater. **6**, 723 (2007).
[2]A. V. Krasheninnikov and K. Nordlund, J. Appl. Phys. **107**, 071301 (2010).
[3]M. C. Hersam, Nat. Nanotechnol. **3**, 387 (2008).
[4]F. Banhart, Rep. Prog. Phys. **62**, 1181 (1999).
[5]A. V. Krasheninnikov, J. Comput. Theor. Nanosci. **5**, 1828 (2008).
[6]T. Stöckli, J. M. Bonard, A. Chatelain, Z. L. Wang, and P. Stadelmann, Appl. Phys. Lett. **80**, 2982 (2002).
[7]Y.-N. Wang and Z. L. Miskovic, Phys. Rev. A **69**, 022901 (2004).
[8]S. W. Chung, D. J. Mowbray, Z. L. Miskovic, F. O. Goodman, and Y.-N. Yang, Radiat. Phys. Chem. **76**, 524 (2007).
[9]I. Radović, L. Hadžievski, N. Bibić, and Z. L. Mišković, Phys. Rev. A **76**, 042901 (2007).
[10]G. Gumbs and A. Balassis, Phys. Rev. B **71**, 235410 (2005).
[11]A. Balassis and G. Gumbs, Phys. Rev. B **74**, 045420 (2006).
[12]S. Segui, J. L. Gervasoni, and N. R. Arista, Radiat. Phys. Chem. **76**, 582 (2007).
[13]J. L. Gervasoni, S. Segui, and N. R. Arista, Radiat. Eff. Defects Solids **162**, 267 (2007).
[14]H. Khosravi, N. Daneshfar, and A. Bahari, Opt. Commun. **281**, 5045 (2008).
[15]M. Z. Herrera and J. L. Gervasoni, Nucl. Instrum. Methods Phys. Res. B **267**, 415 (2009).
[16]M. Inokuti, Rev. Mod. Phys. **43**, 297 (1971).
[17]M. Dapor, L. Calliari, and M. Filippi, Nucl. Instrum. Methods Phys. Res. B **255**, 276 (2007).
[18]C. J. Powell, Surf. Sci. **44**, 29 (1974).
[19]I. Kyriakou, D. Emfietzoglou, R. Garcia-Molina, I. Abril, and K. Kostarelos, Appl. Phys. Lett. **94**, 263113 (2009).
[20]R. Kuzuo, M. Terauchi, and M. Tanaka, Jpn. J. Appl. Phys., Part 2 **31**, L1484 (1992).
[21]R. Kuzuo, M. Terauchi, M. Tanaka, and Y. Saito, Jpn. J. Appl. Phys., Part 2 **33**, L1316 (1994).
[22]A. G. Marinopoulos, L. Wirtz, A. Marini, V. Olevano, A. Rubio, and L. Reining, Appl. Phys. A: Mater. Sci. Process. **78**, 1157 (2004).
[23]R. F. Egerton, *Electron Energy-Loss Spectroscopy in the Electron Microscope* (Plenum, New York, 1996).
[24]M. Inokuti, J. L. Dehmer, T. Baer, and J. D. Hanson, Phys. Rev. A **23**, 95 (1981).
[25]C. T. Chantler, K. Olsen, R. A. Dragoset, A. R. Kishore, S. A. Kotochigova, and D. S. Zucker, online available at http://physics.nist.gov/ffast
[26]G. Bertoni, L. Calmels, A. Altibelli, and V. Serin, Phys. Rev. B **71**, 075402 (2005).
[27]S. Tanuma, C. J. Powell, and D. R. Penn, J. Electron Spectrosc. Relat. Phenom. **62**, 95 (1993).
[28]C. J. Powell and A. Jablonski, J. Phys. Chem. Ref. Data **28**, 19 (1999).
[29]Z.-J. Ding and R. Shimizu, Scanning **18**, 92 (1996).
[30]D. R. Penn, Phys. Rev. B **35**, 482 (1987).
[31]J. C. Ashley, J. Appl. Phys. **69**, 674 (1991).
[32]J. M. Fernández-Varea, R. Mayol, F. Salvat, and D. Liljequist, J. Phys.: Condens. Matter **4**, 2879 (1992).
[33]W. de la Cruz and F. Yubero, Surf. Interface Anal. **39**, 460 (2007).
[34]S. Tanuma, C. J. Powell, and D. R. Penn, Surf. Interface Anal. **37**, 1 (2005).
[35]S. Tanuma, C. J. Powell, and D. R. Penn, Surf. Interface Anal. **25**, 25 (1997).
[36]S. Kamakura, N. Sakamoto, H. Ogawa, H. Tsuchida, and M. Inokuti, J. Appl. Phys. **100**, 064905 (2006).
[37]M. H. Upton, R. F. Klie, J. P. Hill, T. Gog, D. Casa, W. Ku, Y. Zhu, M. Y. Sfeir, J. Misewich, G. Eres, and D. Lowndes, Carbon **47**, 162 (2009).
[38]International Commission of Radiation Units (ICRU), ICRU Report No. 49, 1993 (unpublished).
[39]S. Tanuma, C. J. Powell, and D. R. Penn, J. Appl. Phys. **103**, 063707 (2008).
[40]A. V. Krasheninnikov, Y. Miyamoto, and D. Tomanek, Phys. Rev. Lett. **99**, 016104 (2007).
[41]S. Suzuki and Y. Kobayashi, Chem. Phys. Lett. **430**, 370 (2006).
[42]S. Okada, Chem. Phys. Lett. **447**, 263 (2007).
[43]A. Nojeh, B. Shan, K. Cho, and R. W. W. Pease, Phys. Rev. Lett. **96**, 056802 (2006).
[44]M. K. Alam, S. P. Eslami, and A. Nojeh, Physica E (Amsterdam) **42**, 124 (2009).
[45]M. K. Alam, P. Yaghoobi, and A. Nojeh, Scanning **31**, 221 (2010).

Downloaded 04 Sep 2010 to 195.130.120.61. Redistribution subject to AIP license or copyright; see http://jap.aip.org/about/rights_and_permissions